ELSEVIER

Surface Science 367 (1996) 105–112

surface science

Higher order reconstructions of Pt(110) induced by impurities

I.K. Robinson [a,*], P.J. Eng [a], C. Romainczyk [b], K. Kern [b]

[a] *Department of Physics, University of Illinois, Urbana, IL61801, USA*
[b] *Ecole Polytechnique Fédérale, CH-1015 Ecublens, Switzerland*

Received 5 February 1996; accepted for publication 14 May 1996

Abstract

In the early stages of cleaning a Pt(110) crystal, an interesting series of reconstructions is found to appear, which are attributed to dissolved carbon-based impurities diffusing to the surface. By carefully controlling the preparation conditions while measuring with surface X-ray diffraction, we were able to investigate the structures of these reconstructions and explain them with a simple Hendricks–Teller model. To explain the unusual evolution of the linewidth, we found it necessary to invoke the existence of a new (1×5) local arrangement, intermediate between the previously observed (1×2) and (1×3) phases.

Keywords: Diffusion and migration; Low index single crystal surfaces; Platinum; Surface diffusion; Surface structure, morphology, roughness, and topography; Surface thermodynamics

1. Introduction

There is a long history to the study of the reconstructions of the noble metal surfaces Au(110), Pt(110) and Ir(110), which are known to have "missing row" structures. In all cases, the most commonly reported translational symmetry is (1×2), though (1×3) structures have been reported for both Pt(110) [1–5] and Au(110) [6–11]. Most of these examples of (1×3) structures are due to some deliberate or accidental modification made to the surface [2–6,8–11], but some authors have either claimed the (1×3) to be thermodynamically stable states [1,7] or transient during the preparation [10]. A standard and reproducible way to produce (1×3) structures is by deposition of alkali metal on Au(110) [8], or by bringing Au(110) into equilibrium with an aqueous electrolyte [9], or on strained Au(110) thin films grown epitaxially on Ag(110) [11]. There has also been a previous report of a transient (1×5) structure during cleaning of Pt(110) [12].

Theoretical calculations have demonstrated that there is only a very small free-energy difference between various $(1 \times n)$ structures of Au(110) and Pt(110), or indeed for intermediate stepped configurations of these surfaces [13]. In an earlier study we showed that there is spontaneous step formation associated with the structural phase transition of Pt(110)-(1×2) at 1050 K, which directly implies a vanishing free-energy of step formation at that temperature [14]. Other theoretical studies have found very small values for the step free-energy of certain step geometries [15]. Generally speaking, the favored step geometries are those that expose the most extensive {111} facets, which, being a close-packed face, tend to

* Corresponding author. Fax: +1 217 3336126; e-mail: ikr@uiuc.edu

PII S0039-6028(96)00860-6

have a lower surface free-energy. The higher-order $(1 \times n)$ structures that are favored are similarly the ones with enlarged {111} facets [13]. These may be constructed directly from an initially (1×2) missing-row structure by inserting regular arrays of the right kind of steps in an alternating up-down fashion which preserves the overall (110) orientation of the structure [13].

In this paper we report the observation of a series of incommensurate structures on Pt(110) that change continuously as a function of time after the initial preparation of the clean state. The changes are attributed to impurity segregation. Although we found no fully ordered $(1 \times n)$ states other than the known (1×2) and (1×3), we see strong evidence from the shape of the diffraction that there is a tendency towards a (1×5) structure, which might be made up of alternating (1×2)'s and (1×3)'s, or equivalently, a partially ordered step array in a (1×2) surface.

2. Experimental procedure

Experiments were carried out at beamline X16A at the National Synchrotron Light Source at Brookhaven, USA. The Pt(110) crystal was held in ultra-high vacuum (UHV) on a precision five-circle X-ray diffractometer coupled to the chamber through a bellows and rotating seal [16]. The sample was oriented by means of two out-of-plane bulk Bragg peaks, which defined an orientation matrix in our five-circle diffractometer control program [17]. A tetragonal lattice was chosen to define the unit cell, as previously [5], so that the perpendicular [110] direction was spanned by a single Miller index L The long axis of the tetragonal cell, which is the cubic [001], was spanned by the index h. Automatic settings of arbitrary (h,k,L) points of reciprocal space were then used to scan along high-symmetry directions to look for the reconstruction, which occurs at fractional positions of the index h.

The sample could be monitored in situ with X-ray diffraction at any stage of surface preparation, including the initial cleaning of the crystal. The crystal was expertly polished by U. Linke at KFA Jülich to within 0.1° of the (110) plane, as was verified by aligning the surface normal with a laser beam and comparing this orientation with the crystallographic alignment. Prior to our first experiment, the sample had been cleaned in another UHV system, but had been stored in air in the meantime. The sample was removed and stored in air for several months before our experiment was repeated. The history of the sample and our in situ capabilities were both relevant because observations during cleaning turned out to yield a transient series of interesting new structures.

3. Results and discussion

Fig. 1 shows radial scans taken along $(h,0,0.1)$ in the vicinity of $h = 1.5$, passing through the surface Bragg peak of the (1×2) clean reconstructed surface and the $(1 \times n)$ superstructures too. After introduction in the chamber, the sample was sputtered with Ar^+ ions for 1 h and heated in oxygen for several hours at 500°C, which was found to remove carbon segregating from the bulk. Immediately prior to these measurements, the sample was resputtered, aligned on the diffractometer at 600°C then dosed with oxygen at 2×10^{-7} Torr for a few min until all surface C was removed. Then the peak was scanned repeatedly after the oxygen was shut off. The pressure was less than 3×10^{-10} Torr during the measurements. A clear evolution of the peak position with the length of time spent at 600°C is seen. The changes take place continuously (on the time-scale of a 2 min scan) until a final state is reached when the peak has moved to (1.667,0,0.1), indicating that the surface has transformed from (1×2) to (1×3). After this, no further change was detected over 30 min, so the sample was cooled down so that the (1×3) structure could be determined [5].

The behavior was reversible in the sense that heating in oxygen at 600°C rapidly led to a well-ordered (1×2), and heating without oxygen led slowly to a (1×3). This cycle was repeated twice: the first time leading to a (1×3) in about 5 min, the second (data of Fig. 1) in about 60 min. It could not be repeated again, as a third cycle of oxygen treatment restored the (1×2), but prolonged heating without oxygen did not lead to any

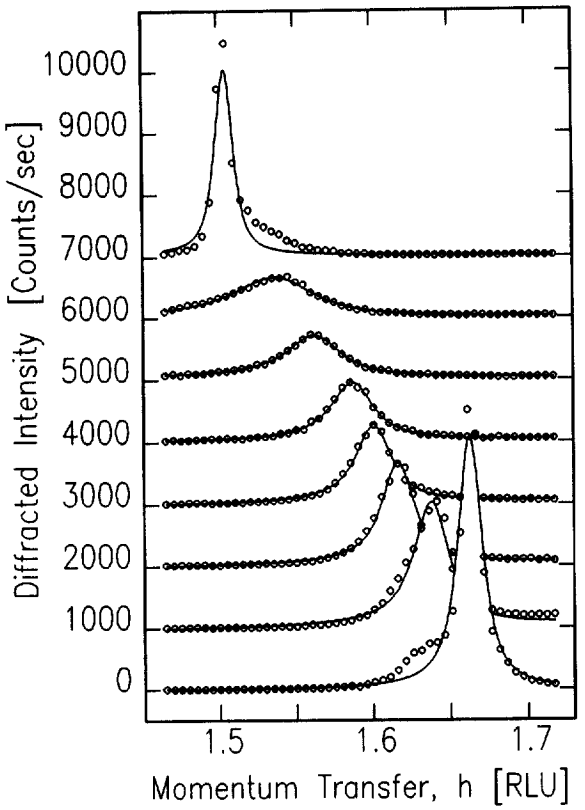

Fig. 1. Radial scans showing the distribution of diffracted intensity in the reconstructed peak as a function of time immediately following oxygen treatment of the sample at 600°C. The solid curves are fits to the Hendricks–Teller model of Eq. (1), with variable fractions of (1×2), (1×3) and (1×5) surface regions. Time runs from top to bottom and the curves have each been offset by 1000 for clarity.

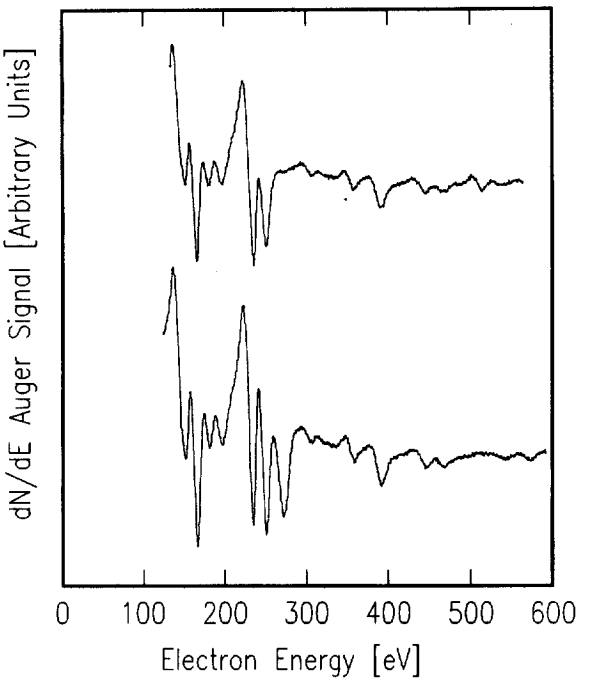

Fig. 2. Auger spectra measured immediately after the second cycle of oxygen treatment when the crystal surface was found to have a (1×2) reconstruction (top) and after the heating experiment described in this paper, when it was found to have a (1×3) reconstruction (bottom). A small oxygen peak (515 eV) can be distinguished in the top curve and a large carbon peak (273 eV) is clearly visible after the structural evolution has taken place.

further change. We concluded that three cycles of oxygen treatment were sufficient to finish cleaning the sample. In a later experiment on the same crystal, having been stored in air for more than one year, we observed exactly the same transient behavior before the sample became clean. Because of the correlation with the early stage of each experiment, we attribute the effect to the segregation of a dissolved impurity, a fact that was readily confirmed by Auger spectroscopy (shown in Fig. 2) at the end of the second heating cycle: a large carbon peak had appeared. Since the impurity returned after exposing the sample to air, it is likely that this corresponds to dissolved atmospheric CO or CO_2.

Between the (1×2) and (1×3) positions, the peak is incommensurate and broad. The width and height of the peak in Fig. 1 change dramatically during the transformation from (1×2) to (1×3). For a preliminary analysis, the changes were documented by fitting a Lorentzian lineshape through each peak and tracking the fit parameters, as shown in Fig. 3. This procedure did not model the slight asymmetries that were present at early and late times, but serves as a guide to the general trends of the data (see below).

The peak is narrow at the two extremes of the trajectory, indicating the pure (1×2) and (1×3) states are both well-ordered. In between, the peak is considerably broader and less tall. The "integrated intensity" shown in Fig. 3, which is simply the peak height multiplied by its width, varies much less across the range. The values at the

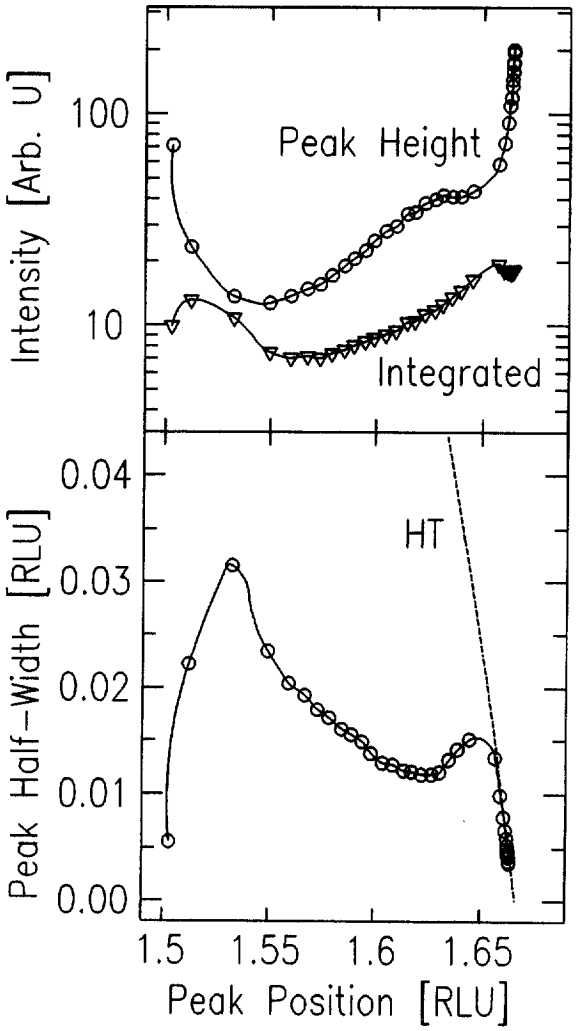

Fig. 3. Peak height and integrated intensity (top) and peak half-width (bottom) as a function of peak position during its evolution with time at 600°C. The points were approximately 2 min apart, with time running left to right. The first point immediately followed the last oxygen dose that was used to clean the sample. The dashed line is the locus of the width and position of the peak obtained with the Hendricks–Teller model for a random mixture of (1 × 3) unit cells in a (1 × 2) structure (see text).

extremes correspond to the squares of the structure factor at (3/2,0,0.1) and (5/3,0,0.1) for the (1 × 2) and (1 × 3) states. The drop in between is suggestive of a disordered state, in which the intensity is spread out in the transverse direction and not fully integrated. Nevertheless, new periodicities are clearly present, since the width is much smaller than the displacement from the ordered positions. This cannot be accounted for by a random mixture of interwoven (1 × 2) and (1 × 3) regions of variable sizes, for example, as we will show next.

We wish to describe a mixed structure containing more than one unit cell length, as applies to our structure which is intermediate between (1 × 2) and (1 × 3). The classical disorder model that derives the characteristic lineshape is due to Hendricks and Teller (HT) [18]. The one-dimensional model assumes a random sequence of unit cells (each with the same form factor) of lengths $L_1, L_2 \ldots L_N$, with probabilities $f_1, f_2 \ldots f_N$, subject to $\Sigma_j f_j = 1$. If q is the momentum transfer, then the average structure will have an average (crystallographic) phase ϕ defined by:

$$\tan\phi = \frac{\sum_j f_j \sin(qL_j)}{\sum_j f_j \cos(qLj)}.$$

The diffracted intensity from this structure is proportional to the expression

$$I(q) = \frac{1-C^2}{1-2C\cos\phi + C^2}, \qquad (1)$$

where

$$C = \sum_j f_j \cos(qL_j - \phi).$$

It can be readily seen by substitution that this expression will give a linear array of sharp Bragg peaks at $q \approx 2\pi n/L_1$ when $f_1 \approx 1$, and at $q \approx 2\pi n/L_2$ when $f_2 \approx 1$, etc. In between these extreme cases (e.g. $f_1 = f_2 = 0.5$), a broad peak is found between the two extreme positions. Similar expressions to Eq. (1) are typically used to describe disorder due to stacking faults in crystals [19] and indeed a similar function was derived to fit LEED spot profiles for Au(110) [20].

Apart from a scale factor, once the N unit-cell lengths are fixed, the only adjustable parameters in Eq. (1) are the probabilities f_j. For an $N = 2$ mixture of just two lengths, $L_1 = 2a_0$ for the (1 × 2) and $L_2 = 3a_0$ for the (1 × 3), $f_2 = 1 - f_1$, so there is only one free parameter. This means that the entire shape of the peak distribution is constrained once the position of its maximum is known. In particu-

lar, the width of the peak is fixed by its position, with the width going to zero at the extremes, $h=3/2$ and $h=5/3$ (in our case). In between the extremes, the width has a locus indicated by the dashed trajectory, denoted "HT" in Fig. 3. This is defined without adjustable parameters and is simply a characteristic of the $N=2$ random case when $L_1=2a_0$ and $L_2=3a_0$. It has the notable property that the full-width of the peak always exceeds its shift. This is a useful criterion that defines the absence of new periodicities.

The data for the observed linewidth obey this theoretical "HT" trend only at the extreme right of Fig. 3, just before arriving at the (1×3) state. It can therefore be claimed that, within this narrow range, the simple $N=2$ HT model describes the data. But the model clearly does not conform with the data elsewhere. Instead, the width turns around and drops to a minimum in the middle of the range, and rises again before reaching the (1×2) position. This behavior indicates there is additional ordering into at least one new structure, with much better ordering than the random mixture of two lengths. One way to explain the data is to consider there to be some preference for alternation of the (1×2) and (1×3) subunits, over the random arrangement. It is notable that in both the top and bottom panels of Fig. 3, the curves turn around near $h=1.6$, where there is a local minimum in the width and local maximum in the height. The rate of shifting does not appear to stop or even slow down, however, and there does not appear to be a tendency towards "locking-in" here. Although this cannot be classified as a fully ordered state, the peak at $h=1.6$ would correspond to a (1×5) structure, perhaps the same state that has been observed in LEED during cleaning of Au(110) by others [10]. We note in addition that the time of appearance of the (1×5) is intermediate between (1×2) and (1×3), suggesting that its structure might also be somehow intermediate.

To verify the arguments for an intermediate (1×5) phase in a quantitative fashion, we then sought to fit the HT model [18] using an explicit (1×5) unit cell, together with the (1×2) and (1×3) cells using $N=3$. We took the unit-cell lengths to be multiples of the bulk lattice parameter, $a_0=3.92$ Å: $L_{(1\times2)}=2a_0$, $L_{(1\times5)}=2.5a_0$ and $L_{(1\times3)}=3a_0$. The incommensurate peak data of Fig. 1 were fitted directly with Eq. (1) using an adjustable scale factor, background and background slope. Since $N=3$, the constraint of $\Sigma_j f_j=1$ means there are two free parameters representing the proportions of the different unit cells mixed together, and so these were fitted without further constraints. The mixture is still completely random, according to the assumptions of the HT model, although the (1×5) unit cell could be thought of as being made up of a bound pair of (1×2) and (1×3) subunits. The results of fitting this five-parameter model are shown as solid curves in Fig. 1. It is clear the model is effective over the full range of data, except where the split peaks occur just next to the commensurate (3/2,0,0.1) and (5/3,0,0.1) positions. The split peaks can be understood to be due to coexisting commensurate and incommensurate phases on the surface, suggesting first-order lock-in transitions (see below). The small detectable shift of the commensurate peaks from the ideal (3/2,0,0.1) and (5/3,0,0.1) positions can be accounted for by residual steps on the surface [14], but we have not tried to account for this in the model, so a bad fit results there. It is particularly noteworthy that the $N=3$ model correctly accounts for the variation of the line widths over the whole range.

The fit parameters $f_{(1\times2)}$, $f_{(1\times5)}$ and $f_{(1\times3)}\equiv 1-f_{(1\times2)}-f_{(1\times5)}$, representing the probabilities of the three unit cells in the HT model, are plotted as a function of time in Fig. 4. The surface starts almost entirely as (1×2) at the beginning, at the moment the oxygen treatment was ended. It then evolves smoothly and rapidly by admixture of (1×5) cells until a maximum probability of $f_{(1\times5)}\approx0.7$ is reached. From that point onwards the (1×3) becomes the dominant minority state and $f_{(1\times3)}$ then rises smoothly to a value of almost 1.0. At each end of the range there is a distortion of the f_j values caused by the poor fitting of the split peaks, and the χ^2 values were found to become large ($\chi^2\approx40$). Elsewhere the χ^2 values were about two up to the middle of the trajectory, and about 20 over the second half when the (1×3) appeared and the peak was larger. Considering the gross simplifications of the model, such as the uniform structure factor for the three phases, this behavior is reasonable.

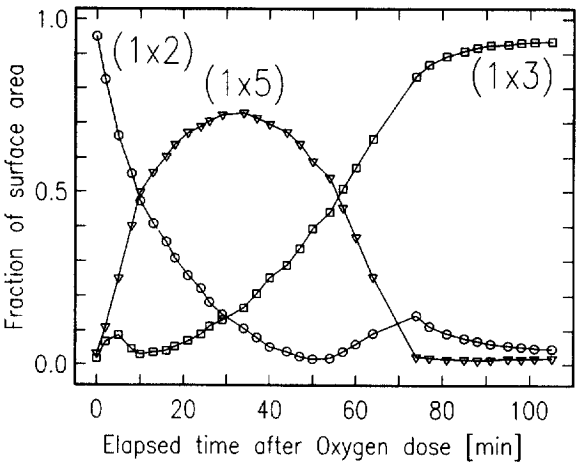

Fig. 4. Time dependence of the Hendricks–Teller fitting parameters, representing the fractions of the surface covered with (1×2), (1×3) and (1×5) regions as indicated. Each sequence of unit cells of different types is assumed to be completely random, according to the Hendricks–Teller model.

4. Conclusions

We now attempt to put the observed transient behavior of this system into context with a physical model. We make the assumption that the impurity segregation, carbon or otherwise, will lead to small changes of the chemical state of the surface, perhaps due to donation or removal of electrons that would change the local surface Fermi level. The thermodynamic state of the system will then be controlled by two variables instead of one: temperature T and chemical potential μ. The chemical potential was not well-controlled in our experiment, as it arose from the accidental segregation process, but it is certainly reasonable to assume that it changes monotonically with time. In principle, μ could be measured as a work-function change, but we did not have the means to do this in our experiment. μ can also be controlled by the deliberate addition of foreign atoms, with alkali metals being an obvious choice, because of their strong charge-transfer and delocalized bonding. An alkali-dosing experiment would be an interesting future extension of this work on Pt(110).

Coverage-dependent structural changes, consistent with this picture of changing chemical potential, have already been observed on other fcc (110) surfaces which are not reconstructed when clean. An alkali-induced series of missing row reconstructions was seen with STM on Cu(110) [21], starting with a (1×3) structure, followed by a (1×2), and then a second (1×3) phase; mixed structures were found in between the well-defined phases. Similar behavior has also been observed for Pd(110) under the influence of hydrogen, which was found to restructure the surface at room temperature [22]. At low hydrogen coverage, these STM measurements revealed a (1×3) missing-row reconstruction. With increasing hydrogen coverage, a two-phase regime with locally coexisting (1×3) and (1×2) reconstructions was passed before a pure (1×2) phase was formed close to monolayer completion [22]. The mixture of missing-row units can thus be regarded as a disordered analog of the (1×5) phase seen here for Pt(110). Potassium was also found to induce structural changes on Pd(110) [23], but the trend was again in the opposite temporal direction from Fig. 1: the LEED peak was broad and situated between the 1/2- and 1/3-order positions at low K-coverage, indicating a disordered (1×2)–(1×3) mixture phase. The peak then narrowed and shifted towards 1/2 during dosing, following a different locus from that seen in Fig. 3, and finally grew into a well-ordered (1×2) phase [23].

We therefore propose the μ–T phase diagram for Pt(110) shown in Fig. 5. The long thick arrow represents the constant-temperature trajectory of the surface during the course of our experiment. We have taken account of the fact that the (1×2) clean surface (for which $\mu=\mu_0$) has a disordering transition at 1050 K [14]. Here we report that the surface departs from the ordered (1×2) state at 870 K once the impurity segregation reaches a certain level, as indicated by the point at which the long arrow crosses the phase boundary at point "A" in Fig. 5. The split peak at early time (Fig. 1) showing (1×2) and incommensurate components suggests that the phase boundary is first-order (see below). After crossing point "A", the system becomes disordered, in the same way as a lattice gas "fluid" phase for an adsorbed gas on a substrate [24]. Point "B" is the closest approach to the putative (1×5) phase, but since this never orders

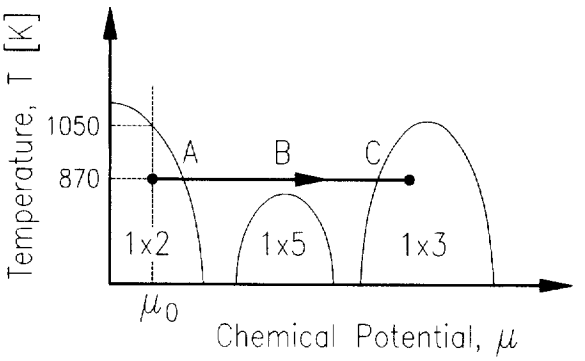

Fig. 5. Notional phase diagram of the Pt(110) surface as a function of temperature T and chemical potential μ as induced by impurity. The locus of structures observed in this experiment is indicated with an arrow. μ_0 is the chemical potential of the clean surface.

completely, we believe that its disordering temperature would be below 870 K. Finally the evolution of the surface proceeds to point "C" where it enters the ordered (1×3) phase, again at an apparently first-order transition.

We should emphasize that we have not identified the thermodynamic phase corresponding to the (1×5) of this phase diagram; its presence is inferred from the partial ordering of the diffuse scattering just outside the proposed phase boundary. Further experiments are needed to verify the existence of the truly ordered thermodynamic phase. Until this is done, we cannot rule out a kinetic mechanism involving competition between various microscopic ordering processes, as an explanation of the narrowing of the diffuse scattering seen in Fig. 3.

Nevertheless we venture to speculate about the atomic arrangement of the proposed intermediate (1×5) state, although this cannot be determined by our measurements of a single structure factor. The (1×2) and (1×3) structures are known to consist of missing-row arrangements derived respectively from the ideal bulk-termination by removal of a single row of atoms or three rows, two in the top layer and one in the second [5]. An obvious hypothesis for the (1×5) structure would be an alternation of these two, but there are (at least) two ways in which this can be constructed, depending on whether the unit cell is considered to start at the top ("ridge") or bottom atom. The STM experiments on Cu(110) [21] imaged boundaries between adjacent regions of (1×2) and (1×3) and found these to be mostly aligned by their ridge atoms, so we might presume that Pt(110) is the same. Other possible structures include much deeper missing-row arrangements. Even though we do not identify the (1×5) atomic structure, we are sure of the existence of a preferred (1×5) periodicity over a random mixture of (1×2) and (1×3). Moreover, if we make the assumption that the (1×5) is indeed made up of an ordered sequence of (1×2) and (1×3) units, this shows there must be an attractive interaction between these units.

There are also other possible explanations of the disorder of the (1×5) structure, which is evident from its broad diffraction peak. By using the HT model, we have assumed it is locally disordered by random mixing of (1×2) and (1×3) unit cells with the (1×5). We further hypothesized that the disorder is thermally induced at 870 K. An alternative explanation of the broad peak might be that there is a series of long-range ordered $(1 \times n)$ states with an inhomogeneous distribution of n across the surface, which might be attributed to spatial variation in the segregation rates, for example. However, we believe that should give rise to lock-in behavior which would manifest itself as multiple peaks in the region of the (1×5) periodicity (in Fig. 1) or else as steps in the peak-width versus position locus (in Fig. 3), neither of which did we see. On the other hand, the peak-splitting seen near the (1×2) and (1×3) positions can be considered to be an example of just this locking-in effect, and the short duration of the coexistence of two peaks there shows that there is relatively little inhomogeneity of the segregating impurity.

The state of reconstruction of a surface can be considered to be a "readout" of the result of optimization of its atomic arrangement to find the lowest free-energy. In consideration of the general thermodynamic problem for the ground state of the surface of a solid, when the total number of atoms need not be conserved, there must be at least two independent variables, a temperature and a chemical potential, which represents the energy cost of adding an atom to the surface from some reservoir (which might be a step-edge, for example). The phase diagram describing such a system must

therefore be at least two-dimensional. Strictly speaking, the bulk chemical potential is a fixed property of every solid element, and cannot be varied at will; systematic studies in chemistry have needed to rely on comparisons between elements to understand the inherent structural trends. A surface is an especially interesting state of matter because of its lower spatial dimension; it offers additional ways to access its chemical potential in a continuous manner, notably by application of an external field (as in electrochemistry) or a small concentration of impurity (as takes place here). The phase diagram of Pt(110) in Fig. 5 summarizes our current understanding of this system. Many details remain to be uncovered by systematic exploration, for example by dosing experiments. We note that there is a specific prediction that an ordered (1×5) phase could be made at lower temperatures by such methods.

Acknowledgements

We have enjoyed fruitful discussions of this work with P. Bak. The work was supported by the US National Science Foundation under grant DMR93-15691. The NSLS is operated by the US DOE under contract DEAC02-76CH00016.

References

[1] P. Fery, W. Moritz and D. Wolf, Phys. Rev. B 38 (1988) 7275.
[2] M. Mundschau and R. Vanselow, Phys. Rev. Lett. 53 (1984) 1084.
[3] M. Stock, J. Risse, U. Korte and G. Meyer-Emsen, Surf Sci. 233 (1990) L243.
[4] F. Masson and J.W. Rabalais, Surf. Sci. 253 (1991) 258.
[5] I.K. Robinson, P.J. Eng, C. Romainczyk and K. Kern, Phys. Rev. B 47 (1993) 10700.
[6] P. Häberle, P. Fenter and T. Gustafsson, Phys. Rev. B 39 (1989) 5810.
[7] G.A. Held, J.L. Jordan-Sweet, P.M. Horn, A. Mak and R.J. Birgeneau, Solid State Commun. 72 (1989) 37.
[8] D.K. Flynn-Sanders, K.D. Jamison, J.V. Barth, J. Winterlin, P.A. Thiel, G. Ertl and R.J. Behm, Surf. Sci. 253 (1991) 270.
[9] B.M. Ocko, G. Hegelsen, B. Schardt, J. Wang and A. Hamelin, Phys. Rev. Lett. 69 (1992) 3350.
[10] W. Moritz and D. Wolf, Surf. Sci. 88 (1979) L79.
[11] Y. Kuk and L.C. Feldman, personal communication.
[12] D. Cvetko, V. de Renzi, L. Floreano, A. Morgante and F. Tommasini, Solid State Commun. 91 (1994) 539.
[13] F. Ercolessi, A. Bartolini, M. Garofalo and E. Tosatti, Surf. Sci. 189/190 (1987) 636.
[14] I.K. Robinson, E. Vlieg and K. Kern, Phys. Rev. Lett. 63 (1989) 2578.
[15] L.D. Roelofs, S.M. Foiles, M.S. Daw and M.I. Baskes, Surf. Sci. 234 (1990) 63.
[16] P.H. Fuoss and I.K. Robinson, Nucl. Instrum. Methods 222 (1984) 171.
[17] E. Vlieg, J.F. van der Veen, J.E. Macdonald and M. Miller, J. Appl. Crystallog. 20 (1987) 330.
[18] S.B. Hendricks and E. Teller, J. Chem. Phys. 10 (1942) 147.
[19] A. Guinier, X-ray Diffraction in Crystals, Imperfect Crystals and Amorphous Bodies (W.H. Freeman, San Francisco, 1963).
[20] D. Wolf, H. Jagodzinski and W. Moritz, Surf. Sci. 77 (1978) 283.
[21] R. Schuster, J.V. Barth, R.J. Behm and G. Ertl, Phys. Rev. Lett. 69 (1992) 2547.
[22] E. Kampshoff, N. Wöchli, A. Menck and K. Kern, to be published.
[23] H. Hörnis and E.H. Conrad, Surf. Sci. 322 (1995) 256 .
[24] E. Bauer, in: Structure and Dynamics of Surfaces II, Eds. W. Schommers and P. von Blanckenhagen (Springer, Heidelberg, 1987) p. 115.